JOURNAL OF
EMERGING INVESTIGATORS

Article

# In silico design of novel acetylcholinesterase inhibitors as potential therapeutics for Alzheimer's disease

**Gia Bao Le[1]*, Kennard Liong[1]*, Artiom Peskur[1], Sopriye Koko[1], Samantha Zhong[1], Porter Beaule[1], Lorcan Purcell[1], Willem Bake[1], Helena Mactier[1], and Carl Sangree[1]**

[1] Northfield Mount Hermon School, Gill, Massachusetts
* These authors contributed equally to this work

## SUMMARY

**Scientific literature suggests that the elevated activity of acetylcholinesterase (AChE) in breaking down the neurotransmitter acetylcholine (ACh) is the main contributing factor leading to cognitive decline and neurodegenerative diseases, including Alzheimer's disease (AD). However, due to the poor bioavailability of existing AChE inhibitors, the demand for new drugs to be developed persists. In this paper, we designed novel, non-toxic, competitive inhibitors targeting AChE from structures of 72 drugs targeting AChE, using computational techniques including molecular docking, chemical analysis, molecular modification, and molecular dynamics (MD) simulation. Since AChE's binding site contains active residues that possess polar aromatic side chains, we hypothesized that adding aromatic R-groups to ligands would promote hydrogen bonding and pi-pi interactions, thereby increasing the thermodynamic favorability of AChE-ligand binding. In accordance with our hypothesis, drugs with high logP (high hydrophobicity) and molar refractivity (high polarizability) had slightly stronger predicted binding energies. In fact, maintaining high logP and molar refractivity, ligands 17 and 18 exhibited the highest predicted binding energies. Moreover, we deemed them as non-toxic toward human cell culture, as they passed the Absorption, Distribution, Metabolism, Excretion, and Toxicity (ADMET) tests. However, when compared to ligand 17 simple chloroethyl side chain, our MD results indicated that bulky or cyclic R-groups in ligand 18 led to less stable binding conformations due to induced steric hindrance in the AChE active site. With these results highlighting the promise of AChE inhibitors, in vivo experiments are required to validate the inhibitory efficacy and cytotoxicity of ligand 17 as a potential-enhanced AD therapeutic.**

## INTRODUCTION

Approximately 6.9 million – 10.9% – of Americans aged 65 and older have AD (1). AD is characterized by progressive memory loss and decline, which are strongly associated with reduced levels of acetylcholine (ACh) in the brain (2). Notably, neuron destruction can start to progress as early as 20 years before showing significant symptoms, including failures in recalling and consolidating memory or maintaining stable mood, to the patients (1). Over time, the neural damage can expand to parts of the brain that are responsible for mobility, ultimately impairing patients' walking, swallowing abilities (1). Such disabilities, compounding worsely over time, cause patients to rely on aid from family relatives to perform daily life activities. Because ACh plays a central role in memory and learning, maintaining its levels is crucial for slowing AD symptoms (3). Acetylcholinesterase (AChE) is an enzyme that catalyzes the inactivation of ACh via the hydrolysis of ACh into acetic acid and choline. This makes AChE a major therapeutic target. As AChE inhibitors can prolong ACh activity in synapses, they help to mitigate the cognitive symptoms of AD (4). Moreover, sustained ACh concentration in synapses supports normal regulation of muscle contractions and autonomic functions, which are often impaired in AD patients (4). Therefore, elevated AChE activity is linked to neurodegenerative disease progression, making the development of a sustainable AChE inhibitor an urgent priority (5).

AChE is a heterodimeric protein that belongs to a family of enzymes called serine hydrolases, known for hydrolyzing peptide bonds using the serine residue in the catalytic site (6). ACh is distributed throughout the central and peripheral systems but is especially prominent in postsynaptic neuromuscular junctions in muscles and nerves (7). The neurotransmitter is degraded by AChE once it finishes carrying the signal from the nerve cell to the muscle cell (7). The active site of AChE contains two subsites: the esteratic and anionic sites. The esteratic site contains a catalytic triad of amino acids—Ser200, His400, and Glu327—that enables AChE to hydrolyze ACh by breaking the ester bond. Meanwhile, the anionic site, composed of Phe330 and Trp84, helps position ACh for catalysis by binding its positively charged quaternary amine (7). Hydrolysis of ACh, eventually, produces acetic acid and choline (7). Additionally, AChE contains peripheral anionic sites (PAS) distinct from the active site that bind quaternary ligands, considered as uncompetitive inhibitors (7). The PAS has attracted attention in drug development, given many AChE inhibitors—such as donepezil-–targets the PAS (8).

The known competitive AChE inhibitors exhibit different inhibitory mechanisms. For example, donepezil acts as a reversible inhibitor; this compound binds non-covalently to the PAS of AChE (8). While reversibility decreases long-term toxicity risk, it also means short-lived inhibition, meaning effectiveness depends heavily on drug concentration (8). As a result, donepezil must be taken regularly to maintain effective drug concentrations, ensuring consistent AChE inhibition and

https://doi.org/10.59720/25-140

sustained acetylcholine elevation (8). Moreover, because donepezil increases ACh broadly, it may cause cholinergic side effects such as nausea, diarrhea, or bradycardia, though its peripheral effects are minimal compared to less selective inhibitors (8). Another inhibitor of AChE, rivastigmine, similarly acts as a slow-reversible inhibitor, binding competitively to the esteratic site of the active site (6). However, unlike donepezil, which selectively inhibits AChE, rivastigmine also targets butyrylcholinesterase (BuChE) (6). Targeting both BuChE and AChE may enhance cholinergic signaling but introduces different drawbacks. For example, BuChE inhibition by rivastigmine raises ACh levels in peripheral tissue, outside the brain, which may contribute to cholinergic side effects (6). Carbamates, on the other hand, are organic compounds characterized by two R-groups derived from carbamic acid (6). These compounds act as reversible AChE inhibitors (6). Despite the diversity of carbamates, the main drawback of these inhibitors is cholinergic toxicity, as excess acetylcholine level can cause confusion, delirium, hallucinations, tremor, and seizures (9). Similarly, donepezil and rivastigmine can also exhibit cholinergic adverse effects, and rivastigmine has limited oral bioavailability (8). These limitations underscore the need for the design of new analogs that maintain AChE inhibition while minimizing off-target cholinergic effects.

To the extent of AChE inhibitors being modified, efforts have been made to better inhibitory efficacy and limit the side-effects of inhibitors. For example, with donepezil, Wang et al. observed an enhanced inhibition through the terminal phenyl ring was substituted with an ortho-fluorophenyl group (10). Moreover, scientists found that donepezil analogs bearing neuroprotective effects when the terminal phenyl ring was replaced by 3-methylpyridinium (10). On the other hand, with carbamate derivative inhibitors, Pizova et. al identified an enhanced inhibition of carbamate derivatives through introducing a chlorine atom at the para-chloro substituent on the anilide phenyl ring (11). They identified that Tyr337, a key residue that shapes AChE's active site gorge, stabilizes ligand binding orientation, thereby enhancing the binding affinity between the drug and AChE active site (11). Ultimately, we hypothesized that the convenience of computational techniques allow us to exploit the modifiability of AChE inhibitors to gain robust insights into AChE-ligand interaction. AChE remains an attractive target for therapeutic intervention due to its high activity in AD patients and its central role in terminating neurotransmission at the cholinergic synapse. Given that currently available AChE inhibitors have bioavailability and toxicity drawbacks, we designed candidate competitive inhibitors with predicted low toxicity for AChE. We docked 72 AChE inhibitors using in-silico techniques to select and modify the one that exhibited the best predicted binding energy. We hypothesized that the more hydrophobic ligands with an aromatic R-group would interact more strongly with available aromatic residues at the AChE binding site through non-polar interactions.

Our data supported our hypothesis, as compounds with high logP–an index of ligand hydrophobicity–and molar refractivity consistently correlate with a favorable binding score. Given that strychnine-derived analogs—i.e., compounds retaining the rigid strychnine core with varied R1 substituents—showed the highest predicted binding energy to AChE among the 13 used scaffolds, future studies should focus on this series. Besides, as MD simulation predicted our best two performing ligands to bind stably to AChE active site, *in vivo* experiments testing the toxicities of these two ligands are required to substantiate their potential as therapeutics.

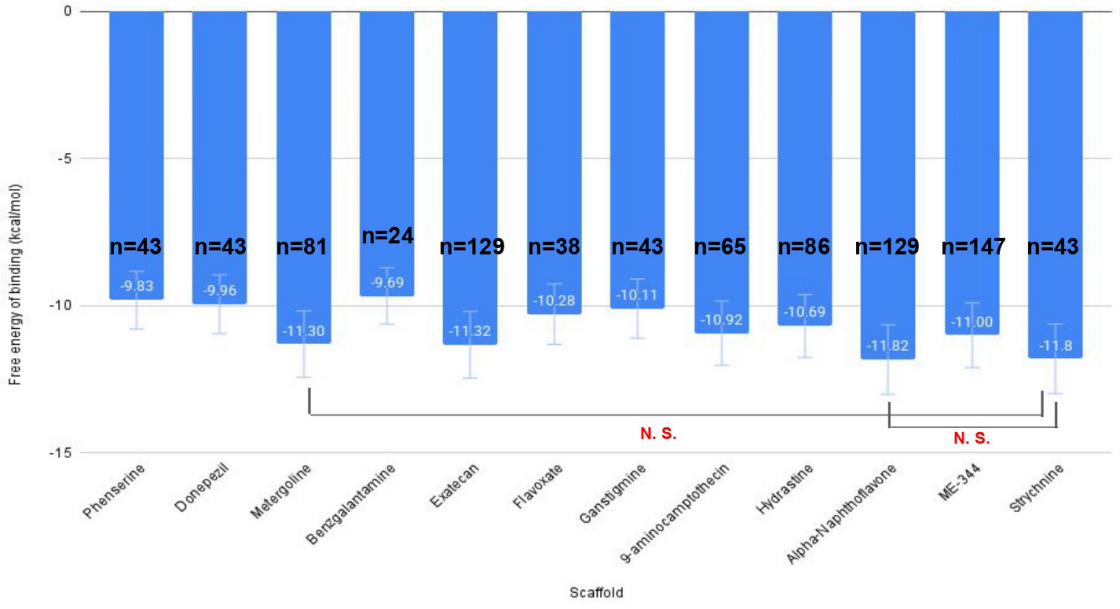


**Figure 1: Mean docking scores for analogs of 13 scaffolds selected out from the initial 72 AChE inhibitors.** Average docking scores for each scaffold are represented by bar groups ± standard deviation of docking scores. N-sample sizes are shown on the bar graphs of each scaffold. Two sample one-tailed t-tests are used to measure statistical significance with a cutoff p-value < 0.05. Statistical insignificant (N. S.) are labelled, while all other comparisons between strychnine, Alpha-Napthoflavone, and Exatecan and the other 11 structures are statistically significant and are not labelled.

https://doi.org/10.59720/25-140

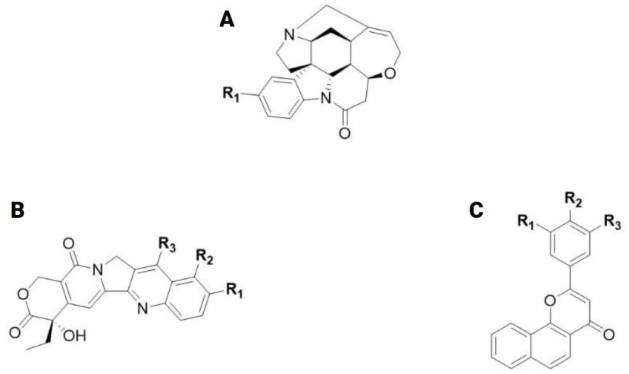


**Figure 2: Top three scaffolds with the highest average docking scores.** A) Common structure of Strychnine analogs. B) Common structure of Exatecan analogs. C) Common structure of alpha-naphthoflavone analogs. Exatecan and alpha-naphthoflavone were shown with three R-groups because their Pubchem analogs were found with three modifiable positions on the scaffold. Strychnine, in contrast, was shown with only one R-group, as its Pubchem analogs only shared one modifiable position. This figure was created in the ChemDraw software.

## RESULTS

### Scaffold analysis and R-group analysis

We compiled a list of structures of 72 existing drugs from Drugbank and selected the top 13 drugs' scaffolds through bash docking. Using a python script, we created 871 analogs of the 13 scaffolds from modifying their R-group(s) and docked them into the active site of AChE. Through Pubchem, we identified positions of R-group(s) on each scaffold through comparing structures of their analogs. From our initial testing, analogs of the 13 best-performing AChE ligands showed varying mean docking scores, ranging from -9.69 ± 0.44 kcal/mol to -11.82 ± 0.77 kcal/mol **(Figure 1)**. Docking score is defined as an index measuring the strength of binding affinity between ligands and AChE, and the lower the score correlates to stronger binding affinity. Analogs of alpha-naphthoflavone had an average docking score of -11.82 kcal/mol, showing the highest predicted binding energy, followed by strychnine (-11.80 kcal/mol) and exatecan (-11.32 kcal/mol) **(Figure 1)**. Two sample one-tailed *t*-tests suggested no significant difference between the mean docking scores of analogs of alpha-naphthoflavone and strychnine (p-value = 0.435), or that of exatecan and metergoline (p-value = 0.419), at a cutoff of α = 0.05 **(Figure 1)**. In contrast, comparisons

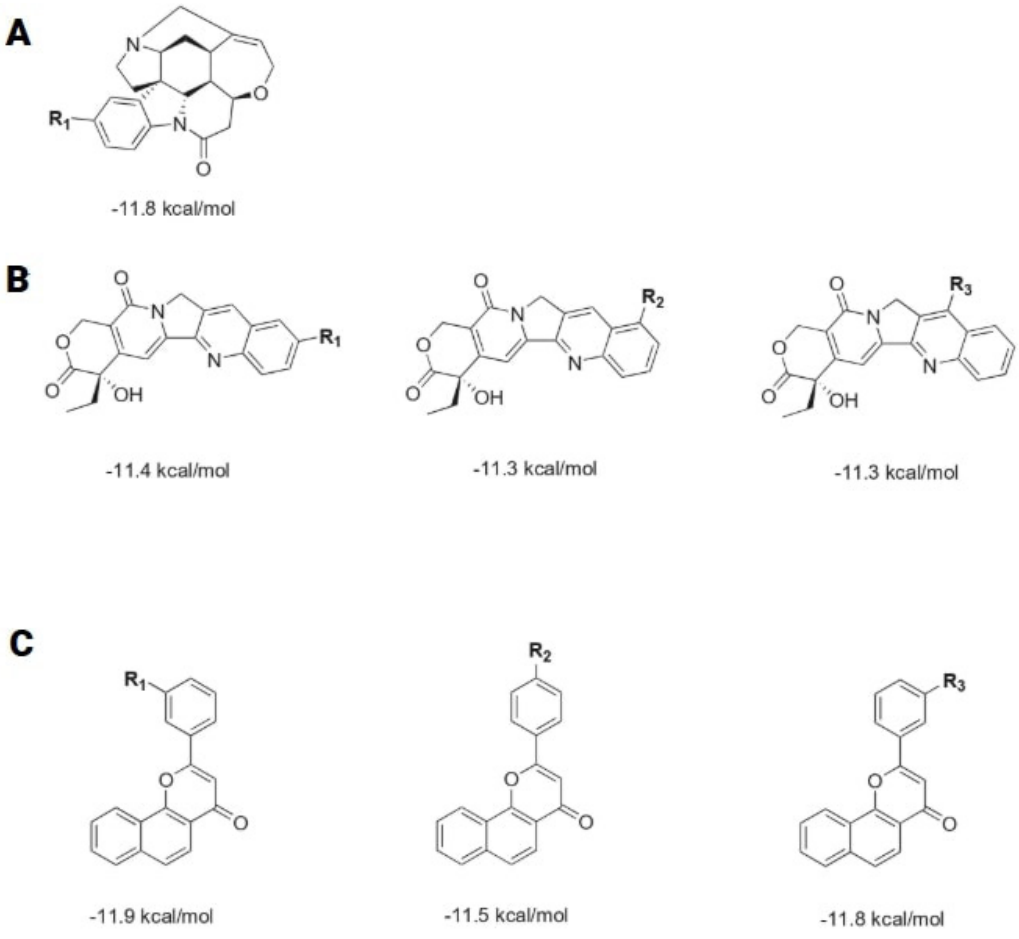


**Figure 3: Average docking scores of structures for the top 3 scaffolds.** The average docking scores (kcal/mol) are shown below the structures. R-groups' positions are found from comparing existing analogs of the scaffold on Pubchem. Each SMILES structure of analogs are created by a Python script, and their docking scores are obtained from bash docking. A) Average docking score for Strychnine's structure. B) Average docking scores for Exatecan's structures. C) Average docking score for alpha-naphthoflavone's structures.

https://doi.org/10.59720/25-140

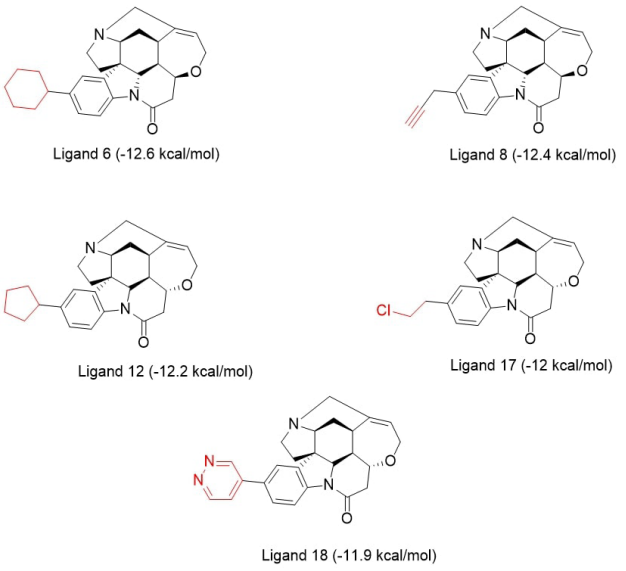


**Figure 4: Chemical structures of the 5 best-performing ligands that are deemed non-toxic in table 1.** The R-group of analogs are colored red. The docking scores (kcal/mol) of each analog are in parentheses.

between the strychnine, alpha-napthoflavone, and exatecan structures and all other structures were statistically significant (p-value < 0.05) **(Figure 1)**. This result suggests heterocyclic structures – found commonly between alpha-napthoflavone, exatecan, and strychnine – exhibit high predicted binding energies to AChE active sites, potentially through induced pi-pi interactions **(Figure 2, 3)**. Given these three structure scaffolds exhibited the highest predicted binding energies, further chemical property analysis and ADMET were performed on 147 analogs of these structures.

## Chemical properties analysis

Prior to chemical property analysis, the chemical structures of the top five best-performing ligands were shown with their R-groups **(Figure 4)**. Chemical property values taken from 147 analogs derived from exatecan-R1, alpha-naphthoflavone-R1, and strychnine scaffolds were arranged into five categories – molecular weight, logP (a measure of hydrophobicity), number of hydrogen bond donors, number of hydrogen bond acceptors, and molar refractivity – and compared against the docking scores of the analogs **(Figure 5)**. LogP and molar refractivity were found to have an inversely proportional relationship with the docking scores **(Figure 5)**, with $R^2$ = 0.259 and 0.18, respectively **(Figure 5)**. Conversely, the number of hydrogen bond donors and acceptors were found to have a proportional relationship with the docking scores, with R2 = 0.089 and 0.15, respectively **(Figure 5)**. No correlation was found between the values of molecular weights and docking scores with R2 = 0.004 **(Figure 5)**. These analyses were made on the assumption that R2 values less than 0.05 were negligible, while those greater than 0.05 were evidence of correlation.

## Pharmacokinetic screening analysis

Out of 147 selected analogs, 20 ligands that passed Lipinski's Rule of Five test and had the lowest docking scores were selected. A ligand, to be considered orally active by Lipkinski's Rule of five, must have molecular weight below 500 Da, logP below 5, numbers of H-bond donors larger than 5, and number of H-bond acceptors larger than 10 (12). From this set of 20 ligands, only the five ligands 6, 8, 12, 17, and 18 passed the toxicity tests conducted through pkCSM webserver. In fact, we deemed these ligands nontoxic due to their negative results in the Salmonella typhimurium reverse mutation assay (AMES), human Ether-a-go-go–Related Gene 1 (hERG I) inhibitor, and hepatotoxicity criteria **(Table 1),** categories measuring toxicity in pkCSM (13). Especially, negative results in hERG I inhibition indicated that these ligands do not inhibit potassium channels, preventing the risk of cardiotoxicity and thus qualify as drug candidates (13). Moreover, the software predicted that all 5 ligands had low water solubility, with values ranging from -4.429 to -2.971 (log mol/L) **(Table 1)** (13). However, it indicated that these ligands had high Caco-2 permeability and intestinal absorption, which were between 1.141-1.187 x $10^{-6}$ cm/s log Papp in and 96.698-100% absorbed, respectively **(Table 1)** (13). Typical values for Caco-2 permeability and intestinal absorption in nontoxic drugs range from log Papp 10 to 70 x 10-6 cm/s, corresponding to ≥ 85-100% absorption in humans (14).The Caco-2 values here (log10 Papp 1.141–1.187 → ~14–15 ×$10^{-6}$ cm/s) and the very high human intestinal absorption (97–100%) fall in the high-permeability/absorption range measured for marketed AChE inhibitors donepezil and rivastigmine The **(Table 1)**. Four out of five ligands were predicted to be moderately toxic given their Lowest Observed Adverse Effect Level (LOAEL) values were in the range of 1-2 (log mg/kg_bw/day). Similarly, rivastigmine was predicted to have a similar LOAEL score of 1.163 **(Table 1)**. In contrast, donepezil and ligand 8 were predicted to be highly toxic given their estimated LOAEL values of 0.991, and 0.832, respectively (log mg/kg_bw/day) **(Table 1)**.

## Analyzing ligand-receptor interactions

We used a molecular docking tool through UCSF Chimera to calculate the docking scores between ACh and strychinine's analogs to AChE. Four docking poses, including ACh, ligand 6, ligand 8, and ligand 12 were analyzed. Ligands 6, 8, and 12 were chosen because of their low docking scores, as they imply thermodynamics favorable binding affinity. Given ligands 6, 8, 12, 17, and 18 share a common strychnine scaffold, we limited our detailed interaction analysis to ligands 6, 8, and 12 to reduce redundancy while still capturing the general interaction trends of the ligands **(Figure 4)**. No hydrogen bonds were observed between AChE and the three analyzed ligands, while there was only one observed in the docking pose of ACh and AChE **(Figure 6)**. However, Van der Waals (VdW) interactions were more commonly observed among molecules with large, bulkier R groups and AChE **(Figure 6)**. This partially explains that the higher binding affinity of ligands 6, 12, and 18 over those with less bulkier R-groups comes from the higher number of VdW interactions existing in their binding pose to AChE **(Figure 4)**.

## Molecular Dynamics (MD) simulations results

Given MD simulations for 20 selected ligands were computationally intensive and went beyond our computational workforce available, we decided to conduct the simulation for ligands 6, 8, 12, 17, and 18 – the top 5 best performing ligands. Among these 5 simulations, convergence, defined

https://doi.org/10.59720/25-140

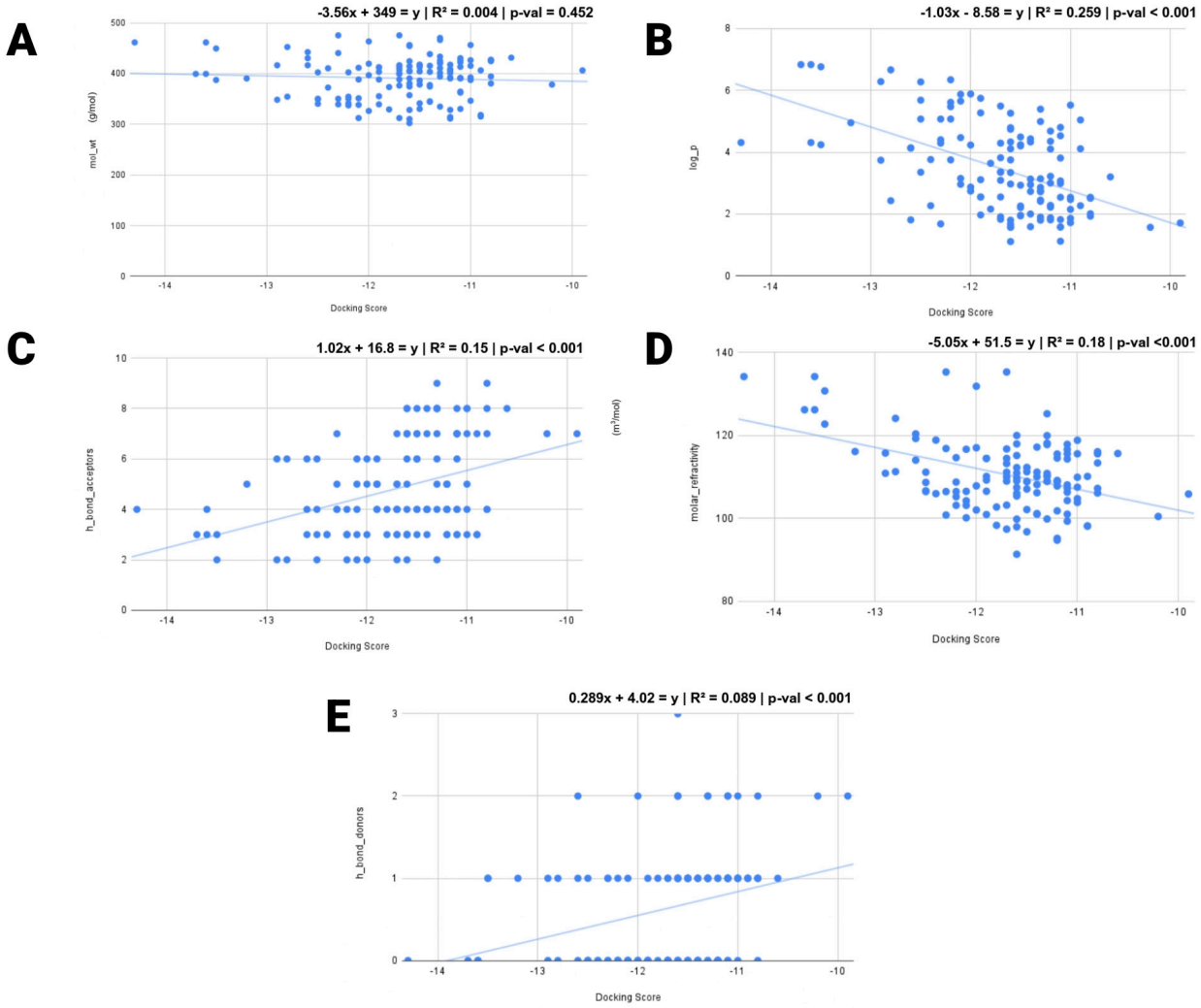


**Figure 5: Chemical property values of 147 analogs derived from exatecan-R1, alpha-naphthoflavone-R1, and strychnine scaffolds.** The chemical property values are plotted on the y-axis, and the docking scores are plotted on the x-axis. Statistical significance correlations (p-value < 0.001) between chemical properties and docking scores are represented through best fit line equations and their associated R2 value, placed above each sub-figure. Docking scores are plotted against (A) molecular weight, (B) logP, (C) Number of hydrogen bonds acceptors, (D) Molar refractivity, (E) Number of hydrogen bond donors. The R2 and p-values were calculated using a significance test for Pearson's correlation coefficient.

as the stabilization of protein backbone Root Mean Square Deviation (RMSD) within ±0.05 nm over the final 20 ns of the trajectory, was observed for ligands 17 and 18, with an equilibrated RMSD of approximately 0.35 nm, 0.45 nm, respectively **(Figure 7).** Further calculations for interacting energies – derived from their Leonard-Jones short-range energy and Coulombic short-range energy – resulted in values of -166.332 ± 4.48 (kJ/mol), -132.483 ± 2.97 (kJ/mol), -163.594 ± 10.5 (kJ/mol), -173.995 ± 6.58 (kJ/mol), and -185.814 ± 14.6 (kJ/mol), for ligand 6, 8, 12, 17, and 18, respectively **(Figure 7)**.

## DISCUSSION

Results showed that the alpha-naphthoflavone and strychnine-derived compounds had the best predicted binding energies, suggesting that the presence of extended conjugation of aromatic rings, which leads to more rigid molecular structures, contribute to stable noncovalent interactions such as pi-pi bonds between the ligand and the aromatic gorge of the AChE protein. In addition, other functional groups on the ligands such as carbonyl or hydroxyl groups, which play a key role as hydrogen acceptors and donors, consolidate the ligand-AChE interactions by fostering the formation of specific hydrogen bonds between ligands and active site residues. As a result, they explain the favorable predicted binding energies of these scaffolds. Compounds that pass criteria placed by Lipinski's Rule of Five are more likely to be orally bioavailable, so we used this filter to select the top 20 drug-like candidates for further analysis. The pharmacokinetic testing for toxicity revealed five of the best-performing non-toxic compounds: ligands 6, 8, 12, 17, and 18, which are all based on strychnine. While there weren't any studies explaining the enhanced binding affinity of analogs derived from strychnine scaffold, we hypothesized that the high rigidity, polycyclic, and non-planar structures of strychnine analogs fit allows them to fit better to the AChE active site gorge. This is evidenced through the success of strychnine analogs to bind strongly to the acyl binding

https://doi.org/10.59720/25-140

| Ligand | Water solubility (log Mol/L) | Caco-2 permeability (log Papp in 10-6 cm/s) | Intestinal absorption (human) (% absorbed) | P-glycoprotein substrate (Yes/No) | Ames toxicity (Yes/No) | hERG I inhibitor (Yes/No) | Lowest observed adverse effect level (LOAEL) (logmg/kg_bw/day) | Hepatotoxicity (Yes/No) |
|---|---|---|---|---|---|---|---|---|
| 1 | -2.892 | 0.952 | 94.153 | Yes | Yes | No | 2.772 | No |
| 2 | -4.454 | 1.271 | 96.615 | Yes | No | No | 1.853 | Yes |
| 3 | -2.903 | 1.3 | 96.579 | Yes | Yes | No | 0.223 | No |
| 4 | -4.696 | 1.277 | 96.79 | Yes | Yes | No | 1.788 | Yes |
| 5 | -3.255 | 1.051 | 95.58 | Yes | No | No | 1.512 | Yes |
| 6 | -4.429 | 1.146 | 98.698 | Yes | No | No | 1.09 | No |
| 7 | -4.179 | 1.265 | 97.192 | Yes | No | No | 1.898 | Yes |
| 8 | -3.488 | 1.162 | 100 | Yes | No | No | 0.832 | No |
| 9 | -4.113 | 1.237 | 100 | Yes | Yes | No | 0.893 | Yes |
| 10 | -5.161 | 0.597 | 95.902 | Yes | Yes | No | 2.978 | Yes |
| 11 | -3.092 | 0.043 | 100 | Yes | No | No | 1.992 | Yes |
| 12 | -4.23 | 1.141 | 98.524 | Yes | No | No | 1.053 | No |
| 13 | -5.818 | 0.535 | 100 | Yes | Yes | No | 0.904 | No |
| 14 | -3.257 | 1.193 | 100 | Yes | No | No | 1.264 | Yes |
| 15 | -5.818 | 0.535 | 100 | Yes | Yes | No | 2.422 | No |
| 16 | -3.709 | 1.136 | 99.441 | Yes | No | No | 1.404 | Yes |
| 17 | -3.764 | 1.147 | 99.305 | Yes | No | No | 1.398 | No |
| 18 | -2.971 | 1.187 | 100 | Yes | No | No | 1.698 | No |
| 19 | -4.035 | 1.334 | 97.486 | Yes | No | No | 1.343 | Yes |
| 20 | -3.145 | 1.009 | 100 | Yes | No | No | 1.486 | Yes |
| RIG | -2.347 | 1.569 | 88.456 | No | No | No | 1.163 | No |
| DON | -4.648 | 1.273 | 93.707 | Yes | No | No | 0.991 | Yes |

**Table 1: Pharmacokinetic properties of the top 20 best performing ligands that passed Lipinski's Rules of Five, Rivastigmine (RIG), and Donepezil (DON).** Water solubility, Caco-2 permeability, human intestinal absorption, and P-glycoprotein substrate status) indicates bioavailability. Ames toxicity, hERG I, lowest observed adverse effect level (LOAEL), and hepatotoxicity indicate the toxicity. Ligands colored in green were deemed non-toxic toward human cell culture. Ligands colored in red were deemed toxic toward human cell culture.

pocket–composed of Phe295, Phe297– of AChE, that other study suggested to be responsible for ligand-specificity (15). These five promising compounds warrant *in vitro* and *in vivo* testing to gauge their potential as drug candidates.

We noted that the presence of aromatic groups in ligand scaffolds seemed to facilitate favorable binding interactions with the AChE protein. This is supported by existing literature on donepezil derivatives in AChE inhibition (10). These derivatives bear structural similarities with strychnine analogs–our best non-toxic performers–with their rigid bicyclic systems and nitrogen-containing cores (10). In addition, the docking results of the ligand-receptors with ligand 6, 12 and AChE indicates enhanced predicted binding energies induced from the pi-pi interaction between the aromatic groups within strychnine analogs and AChE residues Phe338, Tyr341. Aside from the functional groups, the spatial arrangement of this scaffold plays an important role in binding efficiency. With a rigid bicyclic system, strychnine analogs have less conformational flexibility and hence form a more stable interaction with the active site.

Our chemical property values from 147 analogs derived from exatecan-R1, alpha-naphthoflavone-R1, and strychnine scaffolds indicated a weak inversely proportional relationship between logP values and docking scores. This observation was attributed to the equally distributed polar and nonpolar residues in the AChE active site. Since higher logP values correspond to greater hydrophobicity, analogs preferentially engaged in hydrophobic interactions with nonpolar aromatic residues – such as Phe338, Phe295, and Phe297 – while forming VdW and pi-pi interactions with polar aromatic residues – such as Tyr341, Tyr337 – in the active site. Similar to the trend observed with logP, molar refractivity was found to be weakly inversely proportional to the docking scores. Given the higher molar refractivity corresponding to a higher polarizability, analogs with high molar refractivity preferentially engaged in VdW interactions with AChE's active site polar aromatic residues Tyr72, Tyr 124, Tyr337, and Tyr341, leading to an enhanced binding affinity. Besides, numbers of hydrogen bond donors and acceptors were found to be inversely proportional to the docking scores.

https://doi.org/10.59720/25-140

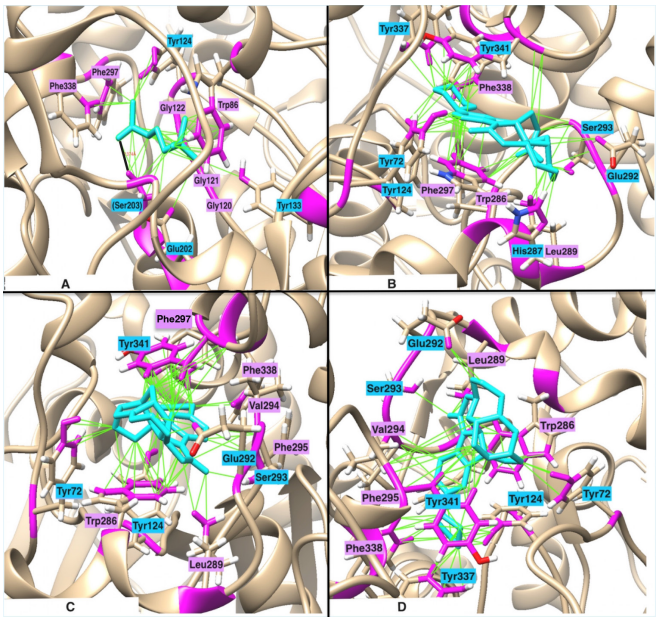


**Figure 6: Binding pose of acetylcholine and best-performing ligands in AChE active site.** Docking poses are visualized through Chimera software. A) ACh docked on AChE. B) Ligand 6 docked on AChE. C) Ligand 8 docked on AChE. D) Ligand 12 docked on AChE. Acetylcholine and ligands are colored cyan; AChE is colored beige; Van der Waals interactions are colored green; hydrogen bonding is colored black; in text, hydrophobic residues are highlighted in pink; hydrophilic residues are blue; residue involving in hydrogen bonding is placed inside a parentheses.

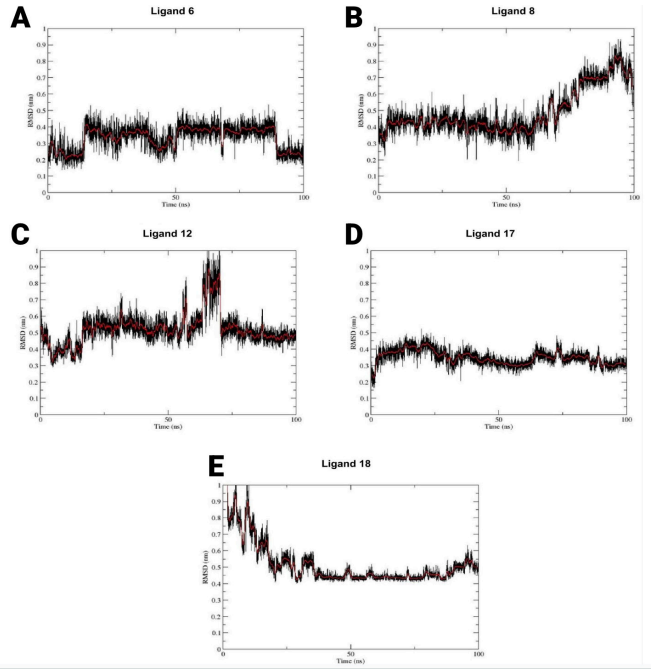


**Figure 7: RMSD of the 5 best-performing non-toxic ligands 6, 8, 12, 17, and 18 against AChE's backbone over 100 ns of MD simulations.** The RMSD values (measured in nm) are plotted on the y-axis, while time (measured in ns) is plotted on the x-axis. The red line represents the smoothed RMSD trends, obtained from the average of 100 data points. A-E) Ligand 6, 8, 12, 17 and 18's RMSD over time with average interacting energies of -166.332 ± 4.48 (kJ/mol), -132.483 ± 2.97 (kJ/mol), -163.594 ± 10.5 (kJ/mol), -173.995 ± 6.58 (kJ/mol), and -185.814 ± 14.6 (kJ/mol), respectively.

This weak correlation was attributed to the desolvation effect caused by the addition of hydrogen bond donors and acceptors in the analogs, leading to a decrease in binding affinity. In addition, only one hydrogen bond was observed across the 4 analyzed docking poses of ACh and ligands 6, 8, and 12 against AChE. This showed that hydrogen bond formation between AChE inhibitors and its active site were generally unfavorable. Moreover, the presence of hydrogen bond donors and acceptors interfered with the formation of VdW and pi-pi interactions, ultimately leading to a decrease in predicted binding energy.

Further ligand-receptor interaction analysis supported the ability of our ligands to inhibit AChE. All three analyzed ligands interacted with Trp286 and Tyr72, two residues on AChE's active site that were responsible for the construction of PAS. Given donepezil primarily binds the PAS of AChE, it was reasonable to hypothesize that our three best-performing ligands share a similar inhibitory mechanism to reversible inhibitors (6). In addition, the acyl pocket, which is composed of Phe295 and Phe297, was reported to be responsible for the binding specificity of ACh to AChE's active site (16). Indeed, our three ligands were shown to fully interact with either Phe295 or Phe297. However, we found that our three ligands bind at different sites with ACh, as they share few interacting residues with each other. Moreover, given our ligands don't interact with any residues composing the ecstatic subsite, which rivastigmine targets, they were hypothesized to have different inhibitory mechanisms (6).

Our MD simulation results indicated ligands 17 and 18 were promising compounds for further drug enhancements. Convergences were only observed on simulations of ligand 17 and 18, and ligand 17 stood out with a low RMSD value at equilibrium of 0.35 nm, which was 0.1 nm shorter than ligand 18's RMSD at equilibrium of 0.45 nm. Ligand RMSD measures how much the ligand's heavy atoms drift from the starting bound pose during the simulation; a lower value means the bound position changed less during the MD run. It does not, by itself, show stronger binding. Ligand 17's propensity to stabilize its interaction earlier to the AChE active site than ligand 18 does implicitly indicates a more stable interaction of ligand 17 to the active site than ligand 18 does. Factors that contribute to the better binding stability of ligand 17 include the structures of these two ligands. Ligand 17 features a relatively small chloroethyl functional group at the para position with respect to the benzyl moiety in the strychnine scaffold; this feature reduced the steric hindrance to allow ligand 17 to bind closer to the active site, contributing to ligand 17's lower RMSD value at equilibrium. On the other hand, the presence of a bulky 1,2-pyridazine functional group at the para position with respect to the benzyl moiety induced more transient reactions in the active site due to its flexibility and polarity, leading to ligand 18's higher RMSD value at equilibration. A higher RMSD value can still be compatible with strong binding if a flexible group moves among nearby positions while keeping favorable contacts. Despite the higher RMSD value, ligand 18 had a more favorable average

https://doi.org/10.59720/25-140

protein–ligand interaction energy than ligand 17, which suggests stronger interactions on average. Lower RMSD value, indicating a more rigid position, and more negative interaction energy, indicating stronger interactions, describe different properties and thus are not contradictory. The fact that ligand 18's simulation yielded a lower overall interacting energy than ligand 17 does indicate ligand 18 had a stronger predicted binding energies to AChE active site than ligand 17. This observation could be attributed to the more potential pi-pi interactions and hydrogen bonding between ligand 18 and the active site than ligand 17. As the 1,2-pyridazine functional group is more flexible and contains two addition nitrogen atoms – which serves as hydrogen bond acceptor – on the benzyl ring than the chloroethyl functional group of ligand 17, ligand 18 was expected to form more VdW interactions and hydrogen bonding in the active site than ligand 17, further leading to a stronger overall interacting energy of ligand 18. Regardless of having a lower interaction energy, ligand 18's interaction with the AChE active site was expected to be less rigid and fluctuate more often than the interaction of ligand 17 with the active site, due to its higher RMSD value at equilibrium when compared to ligand 17's. Therefore, ligand 17 favors positional stability, while ligand 18 favors interaction strength.

Despite the promising results from molecular docking, MD simulation, and pharmacokinetics testing for ligands 17 and 18, relying on these results to conclude the viability of these two compounds in clinical trials is insufficient. Instead, further *in vitro* and *in vivo* experiments are required to validate the efficacy of these two compounds. Thus, isothermal titration calorimetry, surface plasmon resonance, and other *in vitro* experiments assessing and measuring the binding affinity and IC50 values of ligands 17 and 18 to AChE are potential next steps. In addition, other *in vitro* and *in vivo* experiments measuring the blood-brain barrier penetration of ligands 17 and 18 are highly recommended, given their promising predicted bioavailability with high Caco-2 permeability and intestinal absorption. Moreover, *in vivo* studies in animal models are needed to assess toxicity and to determine whether ligands 17 and 18 are viable candidates for clinical trials.

Research into the inhibition of AChE and other neurotransmitter-degrading enzymes is a crucial field for curing neurodegenerative diseases such as AD. Based on our work, future research should focus on designing and testing the inhibitory effects of new strychnine-R1 analogs toward AChE. In addition, given the high binding affinity and stability of ligands 17 and 18 to AChE, future studies can focus on exploring the relationship between the inhibitory efficacy of strychnine-R1 analogs and halogenated, polar aromatic R-groups. While modifying the R-group to include bulkier, nonpolar R-groups induces better predicted binding energy between compounds and the AChE active site, incorporating highly electronegative, small R-groups leads to better binding stability. Doing so will foster robust enhancement in binding affinity of ligands 17 and 18.

Our project highlights the impact of structure-activity-relationship (SAR) analysis. As success in drug modification requires an enormous meta-analysis of SAR analysis, our identification of strychnine as a common scaffold among the initial list of 72 AChE inhibitors and our testing of the inhibitory efficacy of strychnine analogs fits into the bigger picture of finding new AD treatment. We hope our effort in this project will enable scientists to derive better AChE inhibitors from strychnine scaffolds as new AD therapeutics.

## MATERIALS AND METHODS

### Compiling AChE inhibitor analogs for testing

Through the Drugbank website, a library of 72 known inhibitors of AChE was compiled (17). Their structures were compiled from PubChem in a simplified molecular input line entry system (SMILES) (18). These ligands were bash docked, and the top 13 with the lowest docking scores, indicating stronger binding affinity, were further analyzed for their core scaffold structures and R-group modifications. The ligands with the lowest docking scores were used due to their strong predicted binding energy to AChE. The structures for each of the top 13 ligands were compared to similar compounds' structures on PubChem to identify the R-group positions (18). Depending on the number of available R-groups on each scaffold, the number of analogs for them varied **(Figure 1)**. The R-groups on SMILES of each of the top 13 ligands' structures were manually removed, and a Python script was used to attach in these positions functional groups from four categories: aromatic rings, alkyl chains, halogens, and nitrogen-containing groups. From there, those modified analogs were compiled into data sets with their respective 13 initial scaffolds for bash docking.

### Bash docking

The bash docking procedure was carried out in two stages. The initial set of 72 known inhibitors to AChE were in the first trial, while the library of modified compounds derived from structures of 13 best-performing inhibitors from the initial 72 were screened for the second trial. The 3D structure of the AChE enzyme was sourced from the Research Collaboratory for Structural Bioinformatics (RCSB) protein data bank (PDB) in PDB format (PDB ID: 4EY7 for human AChE) (19). Proteins were dock-prepped in UCSF Chimera with Dock Prep, where water molecules and external ligands were removed, and hydrogens and Gasteiger charges were added. Ligand structures were downloaded in Structure-Data File (SDF) format from PubChem and converted to mol2 format. Docking was conducted using Dockstring, a Python package for AutoDock Vina, targeting active residues Phe338, Ser297 and Phe337 in AChE's active site (20, 21). The average docking score was calculated for analogs derived from the structures for the top 13 best performing ligands. To ensure that the selected top three best performing structures were statistically significant, two sample one-tailed *t*-tests were conducted to measure the p-value between the three structures and the other 12 structures **(Figure 1)** (22). Analogs derived from the top three best performing structures with the lowest average docking scores, implying highest ligand-AChE affinity interaction, were compiled and assessed according to Lipinski's Rules of Five via a Python script. Each rule (molecular weight, logP, number of hydrogen bond donors, and number of hydrogen bond acceptors) in Lipinski's Rules of Five were weighted equally. That is, a ligand would be considered to fail the test if it violated one out of the four rules. The top 20 ligands that passed the Lipinski's Rules of Five tests were isolated and underwent the pharmacokinetic property analysis.

https://doi.org/10.59720/25-140

### Chemical property analysis

After docking, ligands were assessed for chemical properties, including molecular weight, Wildman-Crippen log partition coefficient (logP), hydrogen bond donors and acceptors, rotatable bonds, aromatic ring count, molar refractivity, and topological polar surface area (TPSA), using the RDKit Python package. Correlations between molecular properties and predicted binding energies of ligands, represented through their docking scores (with more negative values indicating stronger binding affinity), were visualized through scatter plots. Through Google Sheets correlation (CORREL) and t-distribution (TDIST), significance tests for Pearson's correlation coefficient were performed to calculate the R2 and p-value between analogs' chemical properties and their docking scores, with a cutoff of p-value < 0.05 (22). For chemical property analysis, R2 values less than 0.05 were deemed negligible, while R2 values greater than 0.05 were deemed to be evidence of correlation.

### Pharmacokinetic property analysis

Pharmacokinetic characteristics such as water solubility (log Mol/L), Caco-2 permeability (log Papp in 10^-6 cm/s), human intestinal absorption (% absorbed), P-glycoprotein substrate status, Ames toxicity, human ether-à-go-go related gene (hERG) I inhibition, lowest observed adverse effect level (LOAEL), and hepatotoxicity predictions were determined using the pkCSM web server for the top 20 ligands isolated from the bash docking section (13). Intestinal absorption, a critical first step that determines bioavailability for orally administered drugs, was reflected by Caco-2 permeability index. P-glycoprotein (P-gp) substrate status was evaluated, given P-gp efflux can reduce the intracellular retention and thus lower the bioavailability. Lastly, hERG I inhibition criteria indicate the risk of cardiotoxicity, which results as a consequence of inhibiting potassium channels.

### Visualization of docking poses and ligand-receptor interactions

Given lower docking scores imply higher binding affinity, 4 docking poses of ACh and ligands 6, 8, and 12 were visualized using UCSF Chimera (v1.17.3) (23). Hydrogen bonds were identified within a 4.0Å proximity between ligands and receptor residues. Van der Waals interactions were evaluated using a −0.4Å cutoff. Resides in AChE active sites involving interaction with ACh and best performing ligands were highlighted according to the polarity.

### MD simulation

Given MD simulations for 20 selected ligands were computationally intensive and went beyond our computational workforce available, we decided to conduct the simulation for ligands 6, 8, 12, 17, and 18 – the top 5 best performing ligands with lowest docking scores. These simulations were conducted through GROMACS-2024.3 – an open-access software (24). AChE-ligand complexes were separated and prepared independently with respect to the CHARMM36 forcefield (25). AChE's CHARMM parameter was prepared by the pdb2gmx module in GROMACS with the N-, C-termini charged as "NH3+" and "COO-", respectively (24). The ligand's parameter was obtained from the CGenFF web server (26). Ligands with parameters having either param or charge penalties exceeding 50 underwent optimization in Orca 5.0, in which the density functional theory with the B3LYP and def2-TZVP basis sets was employed for a reliable geometry optimization (27-29). This setting was aided by the TightOpt and TightSCF modules, which aim to ensure a more rigorous geometry optimization and charge distribution, respectively (27). After force field preparations, the ligand topology file was manually incorporated into the AChE topology file, reforming the AChE-ligand complex. The complex was solvated in a cubic water box, neutralized with counterions, and energy was minimized with the steepest descent method (24). Equilibration was performed under Canonical (NVT) and Isothermal-Isobaric (NPT) ensembles in 10 ps, aiming to stabilize the pressure and temperature of the system to 1 bar and 300k, respectively (24). Then, the AChE-ligand complex underwent a 100 ns MD simulation, in which RMSD analysis was used to keep track of the distance between ligands and AChE's backbone. In addition, the Leonard-Jones short-range energy and Coulombic short-range energy were measured to calculate the total interacting energies for each system (30).

**Received:** March 7, 2025
**Accepted:** October 29, 2025
**Published:** January 22, 2026

## REFERENCES

1. Alzheimer's Association. "2024 Alzheimer's Disease Facts and Figures." *Alzheimer's & Dementia*, vol. 20, no. 5, 2024, https://doi.org/10.1002/alz.13809.
2. Rees, T. M., Brimijoin, S. "The Role of Acetylcholinesterase in the Pathogenesis of Alzheimer's Disease." *Drugs of Today,* vol. 39, no. 1, 2003, https://doi.org/10.1358/dot.2003.39.1.740206.
3. Jorm, Anthony F. "Effects of Cholinergic Enhancement Therapies on Memory Function in Alzheimer's Disease: A Meta-Analysis of the Literature." *Australian & New Zealand Journal of Psychiatry*, vol. 20, no. 2, 1 June 1986, pp. 237–240, https://doi.org/10.3109/00048678609161337.
4. McGleenon, B. M., et al. "Acetylcholinesterase Inhibitors in Alzheimer's Disease." *British Journal of Clinical Pharmacology,* vol. 48, no. 4, 2001, https://doi.org/10.1046/j.1365-2125.1999.00026.x.
5. Trang, Amy and Paras Khandhar. *Physiology, Acetylcholinesterase*. PubMed. https://doi.org/10.1038/35067589.
6. Colovic, Mirjana, et al. "Acetylcholinesterase Inhibitors: Pharmacology and Toxicology." *Current Neuropharmacology*, vol. 11, no. 3, 2013. https://doi.org/10.2174/1570159x11311030006.
7. Zhou, Yanzi, et al. "Catalytic Reaction Mechanism of Acetylcholinesterase Determined by Born−Oppenheimer Ab Initio QM/MM Molecular Dynamics Simulations." *The Journal of Physical Chemistry B*, vol. 114, no. 26, 2010. https://doi.org/10.1021/jp104258d.
8. Thompson, Sarah, et al. "The Benefits and Risks Associated with Cholinesterase Inhibitor Therapy in Alzheimer's Disease." *Expert Opinion on Drug Safety*, vol. 3, no. 5, 2004. https://doi.org/10.1517/14740338.3.5.425.
9. Silberman, Jason, and Alan Taylor. "Carbamate Toxicity." National Library of Medicine, *StatPearls Publishing*, May 2023, www.ncbi.nlm.nih.gov/books/NBK482183/.
10. Wang, Zhi-Min, et al. "Rational Modification of Donepezil as Multifunctional Acetylcholinesterase Inhibitors for the

https://doi.org/10.59720/25-140

Treatment of Alzheimer's Disease." *European Journal of Medicinal Chemistry*, vol. 123, 2016. https://doi.org/10.1016/j.ejmech.2016.07.052.
11. Pizova, Hana, et al. "Proline-Based Carbamates as Cholinesterase Inhibitors." *Molecules*, vol. 22, no. 11, 2017. https://doi.org/10.3390/molecules22111969.
12. Benet, Leslie Z, et al. "BDDCS, the Rule of 5 and Drugability." *Advanced Drug Delivery Reviews*, vol. 101, 13 May 2016, pp. 89–98. https://doi.org/10.1016/j.addr.2016.05.007.
13. Pires, D. E. V., et al. "PkCSM: Predicting Small-Molecule Pharmacokinetic and Toxicity Properties Using Graph-Based Signatures." *Journal of Medicinal Chemistry*, vol. 58, no. 9, 2015. https://doi.org/10.1021/acs.jmedchem.5b00104.
14. Press, Barry, and Deanna Di Grandi. "Permeability for Intestinal Absorption: Caco-2 Assay and Related Issues." *Current Drug Metabolism*, vol. 9, no. 9, 1 Nov. 2008. https://doi.org/10.2174/138920008786485119.
15. Hung, Li-Wei, et al. "Acetylcholinesterase: Structure, Dynamics, and Interactions with Organophosphorus Compounds." *Protein Science*, vol. 34, no. 10, 19 Sept. 2025, https://doi.org/10.1002/pro.70297.
16. K.V. Dileep, et al. "Crystal Structure of Human Acetylcholinesterase in Complex with Tacrine: Implications for Drug Discovery." *International Journal of Biological Macromolecules*, vol. 210, 6 May 2022. https://doi.org/10.1016/j.ijbiomac.2022.05.009.
17. Knox, Craig, et al. "DrugBank 6.0: The DrugBank Knowledgebase for 2024." *Nucleic Acids Research*, vol. 52, no. D1, 11 Nov. 2023, pp. D1265–D1275, https://doi.org/10.1093/nar/gkad976.
18. Kim, Sunghwan, et al. "PubChem 2025 update." *Nucleic Acids Research*, vol. 53, 6 Jan. 2025, https://doi.org/10.1093/nar/gkae1059.
19. Berman, H. M. "The Protein Data Bank." *Nucleic Acids Research*, vol. 28, no. 1, 2000. https://doi.org/10.1093/nar/28.1.235.
20. Eberhardt, J., et al. "AutoDock Vina 1.2.0: New Docking Methods, Expanded Force Field, and Python Bindings". *Journal of Chemical Information and Modeling*, *vol. 61, no. 8, 2021*. https://doi.org/10.1021/acs.jcim.1c00203.
21. Trott, O. and Oleg Olson "AutoDock Vina: Improving the Speed and Accuracy of Docking with a New Scoring Function, Efficient Optimization, and Multithreading." *Journal of Computational Chemistry*, vol 31, no. 2, 2009. https://doi.org/10.1002/jcc.21334.
22. Student. "The Probable Error of a Mean." *Biometrika*, vol. 6, no. 1, 1908, pp. 1-25., https://doi.org/10.2307/2331554.
23. Pettersen, E. F., et al. "UCSF Chimera--a Visualization System for Exploratory Research and Analysis." *Journal of Computational Chemistry*, vol. 25, no. 13, 2004. https://doi.org/10.1002/jcc.20084.
24. Van Der Spoel, D., et al. "GROMACS: Fast, Flexible, and Free." *Journal of Computational Chemistry*, vol. 26, no. 16, 2005. https://doi.org/10.1002/jcc.20291.
25. Brooks, B. R., et al. "CHARMM: The Biomolecular Simulation Program." *Journal of Computational Chemistry*, vol. 30, no. 10, 2009. https://doi.org/10.1002/jcc.21287.
26. Vanommeslaeghe, K. and Alexander MacKerell Jr. "Automation of the CHARMM General Force Field (CGenFF) I: Bond Perception and Atom Typing." *Journal of Chemical Information and Modeling*, vol. 52, no. 12, 2012. https://doi.org/10.1021/ci300363c.
27. Neese, F. Software Update: "The ORCA Program System—Version 5.0." *WIREs Computational Molecular Science*, vol. 12, no. 5, 2022. https://doi.org/10.1002/wcms.1606.
28. Becke, A. D. "Density-Functional Thermochemistry. III. The Role of Exact Exchange." *The Journal of Chemical Physics*, vol. 98, no. 7, 1993. https://doi.org/10.1063/1.464913.
29. Weigend, F. and Reinhart Ahlrichs**.** "Balanced Basis Sets of Split Valence, Triple Zeta Valence and Quadruple Zeta Valence Quality for H to Rn: Design and Assessment of Accuracy." *Physical Chemistry Chemical Physics*, vol. 7, no. 18, 2005. https://doi.org/10.1039/b508541a.
30. MacKerell, A. D., et al. "All-Atom Empirical Potential for Molecular Modeling and Dynamics Studies of Proteins." *The Journal of Physical Chemistry B*, vol. 102, no. 18, 1998. https://doi.org/10.1021/jp973084f.

https://doi.org/10.59720/25-140

## APPENDIX

Github repository for used scripts: https://github.com/kennardliong/ache-paper-scripts